

Least-Square Fit, Ω Counters, and Quadratic Variance

F. Vernotte[⊓], M. Lenczner[∇], P.-Y. Bourgeois[∇], E. Rubiola[∇]

⊓ UTINAM/Observatory THETA, University of Franche-Comté and CNRS,
41 bis, avenue de l'observatoire, BP 1615, 25010 Besançon Cedex, France

∇ FEMTO-ST Institute, UMR 6174 : CNRS/ENSMM/UFC/UTBM, Time and Frequency Dpt.,
26 ch. de l'Épitaphe, 25030 Besançon Cedex, France

Abstract—This work is motivated by the wish to have the most precise measurement of a frequency ν and of the variance σ_y^2 of its fractional fluctuations in a given time τ , out of high-end general-purpose instruments.

Thanks to the progress of digital electronics, new time-interval analyzers have been made available in the last few years. Such instruments measure the time stamp of the input events at high sampling speed (MS/s), and with high resolution (10–100 ps).

We propose the linear regression as a means to estimate the frequency from time stamps of the input signal. The frequency counter based on the linear regression is called Ω counter. The linear regression is interpreted as a finite impulse response filter which takes the frequency samples as the input, and delivers the estimated frequency at the output. We derive the transfer function of such filter, which turns out to be parabolic shaped. As compared to the Π and Λ counters, the Ω counter features better rejection of the background noise.

We define the quadratic variance (QVAR), a wavelet variance similar to the Allan variance, and we derive its statistical properties. The QVAR is superior to the AVAR and MVAR in the rejection of the background noise.

I. THE Ω COUNTER

For our purposes, the time analyzer takes the input signal as the ‘start,’ and the reference as the ‘stop,’ and also as the time stamp. Let us assume that reference signal (stop) has frequency $1/\tau_0$, that input signal (start) has the nominal frequency ν_0 , and that ν_0 is greater or equal than the sampling frequency $1/\tau_0$. In this conditions, at each ‘stop’ event the instrument measures the time interval $t_{\text{stop}} - t_{\text{start}}$. The time tag associated to the measure is t_{stop} . Broadly speaking, this is equivalent to the ‘Picket Fence’ scheme introduced by Greenhall [1], [2].

We define the *phase time*, denoted with x , as either $t_{\text{stop}} - t_{\text{start}}$ or its fluctuation. Similarly, we define the fractional frequency y either as ν/ν_0 or its fluctuation $(\nu - \nu_0)/\nu_0$. Of course, the use of ‘value’ and ‘fluctuation’ must be consistent.

We introduce the Ω counter as a new type of frequency counter that uses the linear regression on the time series $\{x_k\}$ as the means to estimate the input frequency. Presently, the Ω counter is a proposed implementation using time-tag time interval counters. The game of the name Ω will be explained later.

General purpose time-tag instruments have wide input bandwidth (usually 0.2...2 GHz, or more), thus the instrument background is chiefly white noise, with negligible contribution

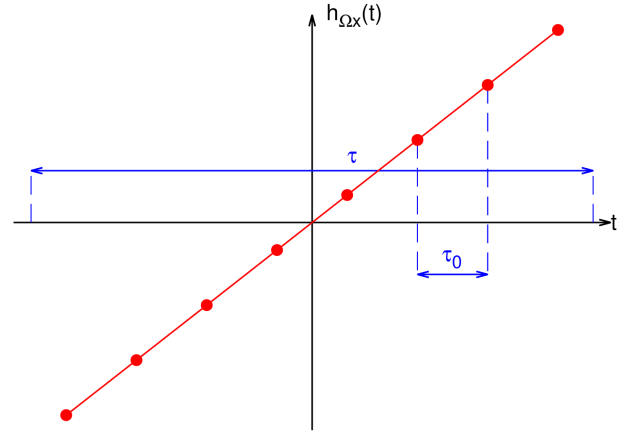


Figure 1. The linear regression estimator

of flicker and other coloured noise types. In this conditions, the linear regression is an obvious choice as it gives the best rejection of the background.

Let us denote with $\mathcal{A} = \nu/\nu_0$ either the fractional frequency or its fluctuation, and with $\tilde{\mathcal{A}}$ its estimate. Using the linear regression in the time interval $\tau = N\tau_0$ centered at $t = 0$, $\tilde{\mathcal{A}}$ reads

$$\tilde{\mathcal{A}} = \frac{12}{N^3\tau_0^2} \sum_{k=-(N-1)/2}^{(N-1)/2} k x_k. \quad (1)$$

Equation (1) gives the fractional frequency when we take $x = t_{\text{stop}} - t_{\text{start}}$, and its fluctuation when we take x as the fluctuation or the background noise.

A. Phase-time filter interpretation

We rewrite Equation (1) as

$$\tilde{\mathcal{A}} = \sum_k h_{\Omega x}(t_k) x_k, \quad (2)$$

where

$$h_{\Omega x}(t) = \frac{12t}{\tau^3} = \frac{12t}{N^3\tau_0^3} \quad (\text{Fig. 1}) \quad (3)$$

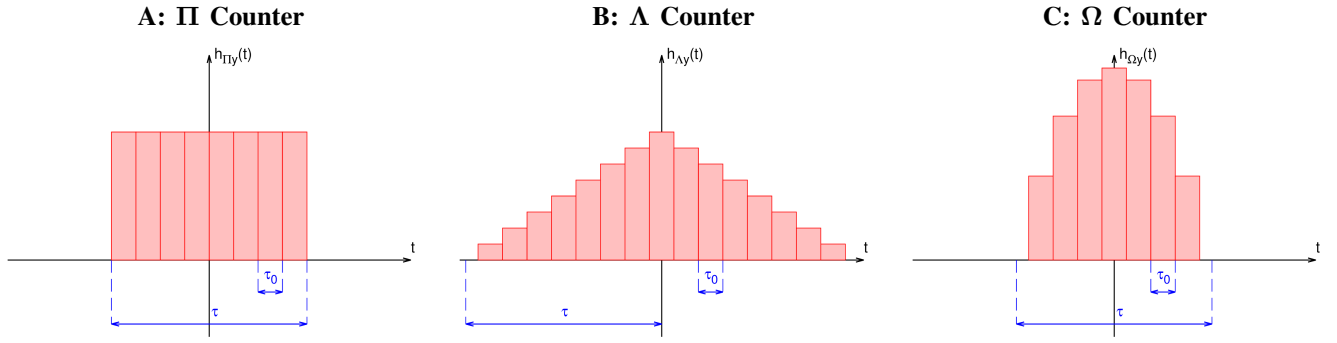


Figure 2. Weight function of the Π , Λ and Ω counters.

Equation (2) states that the linear regression can be interpreted as a *filter* applied to the phase-time data. Alternatively, the linear regression can be seen as a *weighted measure*. This alternate interpretation is made easy by the symmetry of $h_{\Omega x}$.

B. Frequency filter interpretation

We rewrite Equation (1) as

$$\tilde{A} = \sum_k h_{\Omega y}(t_k) y_k \quad (4)$$

where $h_{\Omega y}(t)$ is given by

$$h_{\Omega x}(t) = \frac{d}{dt} h_{\Omega y}(t), \quad (5)$$

thus

$$h_{\Omega y}(t) = \frac{6}{\tau^3} \left(\frac{\tau^2}{4} - t^2 \right). \quad (\text{Fig. 2 C}) \quad (6)$$

Equations (4)–(6) rely on the property of the convolution integral, that $f' * g = f * g'$.

As before, the linear regression can be interpreted as a *filter*. However, the filter now processes the *fractional frequency* $\{y_k\}$ associated to $\{x_k\}$, and delivers the estimated frequency. The impulse response of such filter is $h_{\Omega y}$. Alternatively, the linear regression is seen as a weighted measure applied to $\{y_k\}$. The relation between these two interpretations is made easy by the symmetry of $h_{\Omega y}$.

C. The game of the name

In a previous paper [3] we introduced terms ‘ Π counter’ and ‘ Λ counter’ for the instruments with rectangular and triangular weight function, respectively. In the same way we use the term ‘ Ω counter’ for the linear-regression counter, because the impulse response has parabolic shape, which is broadly similar to the Greek letter Ω (Fig. 2 C).

II. COMPARISON OF THE Π , Λ AND Ω COUNTERS

We introduce two classical operators, the mathematical expectation $\mathbb{E}\{x\}$, and the mathematical expectation of the variance $\mathbb{V}\{x\} = \mathbb{E}\{[x - \mathbb{E}\{x\}]^2\}$ of a random variable x .

Figure 2 shows the weight functions of the Π counter, the Λ counter, and the new Ω counter. We compare the performance

Table I
 Π , Λ AND Ω COUNTERS IN THE PRESENCE OF WHITE PM NOISE

| Π counter | Λ counter | Ω counter |
|--|--|--|
| Support τ | Support 2τ | Support τ |
| $\mathbb{E}\{\tilde{\mathcal{A}}_{\Pi}\} = \nu/\nu_0$ unbiased estimate | $\mathbb{E}\{\tilde{\mathcal{A}}_{\Lambda}\} = \nu/\nu_0$ unbiased estimate | $\mathbb{E}\{\tilde{\mathcal{A}}_{\Omega}\} = \nu/\nu_0$ unbiased estimate |
| $\mathbb{V}\{\tilde{\mathcal{A}}_{\Pi}\} = \frac{2\sigma_x^2}{\tau^2}$ | $\mathbb{V}\{\tilde{\mathcal{A}}_{\Lambda}\} = \frac{2\tau_0\sigma_x^2}{\tau^3}$ | $\mathbb{V}\{\tilde{\mathcal{A}}_{\Omega}\} = \frac{12\tau_0\sigma_x^2}{\tau^3}$ |

of these counters in the presence of white PM noise with zero mean and variance σ_x^2 . Basic statistics (details are omitted) gives the results summarized in Table I.

The Π counter is clearly inferior to the other two because the white PM noise is rejected as $1/\tau^2$ instead of $1/\tau^3$. The Λ looks superior to the Ω counter only because the measurement is allowed to take twice the time. If we constrain the measurement time to τ for both, we get

$$\mathbb{V}\{\tilde{\mathcal{A}}_{\Lambda}\} = \frac{16\tau_0\sigma_x^2}{\tau^3} = \frac{4}{3}\mathbb{V}\{\tilde{\mathcal{A}}_{\Omega}\}. \quad (7)$$

The supports are chosen for the two-sample variance (defined later) to be the same for the three counters.

III. THE TWO SAMPLE VARIANCE

The two-sample variance is defined as

$$\sigma_y^2 = \frac{1}{2}\mathbb{E}\{(y_2 - y_1)^2\}, \quad (8)$$

where y results from the appropriate estimator. We get the Allan variance AVAR with $y = \mathcal{A}_{\Pi}$ (Π estimator), the modified Allan variance MVAR with $y = \mathcal{A}_{\Lambda}$ (Λ estimator), and the new quadratic variance QVAR with $y = \mathcal{A}_{\Omega}$ (Ω estimator).

IV. THE QUADRATIC VARIANCE QVAR

A. Time domain

Using phase measurements as the input data, the QVAR is given by

$$\sigma_Q^2(\tau) = \left\langle [x(t) * h_{Qx}(t)]^2 \right\rangle \quad (9)$$

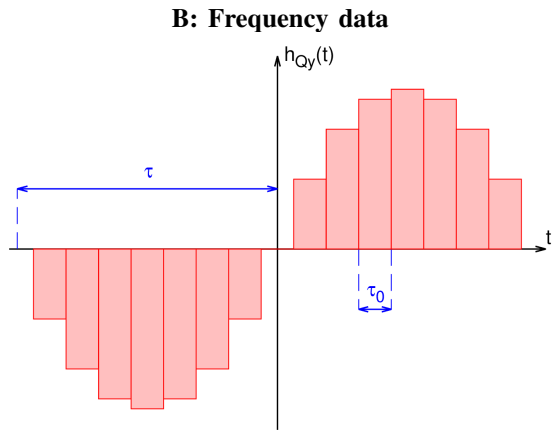
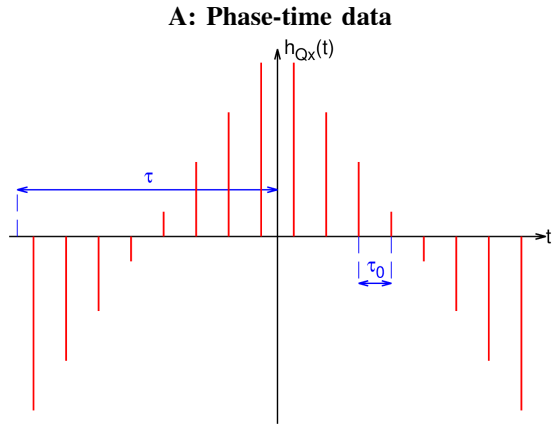


Figure 3. Time domain computation weight of QVAR for phase data (above) or frequency deviations (below).

with (Fig. 3-A)

$$h_{Qx}(t) = \frac{6\sqrt{2}}{\tau^3} \left(t + \frac{\tau}{2} \right) \quad t \in [-\tau, 0[$$

$$= \frac{6\sqrt{2}}{\tau^3} \left(-t + \frac{\tau}{2} \right) \quad t \in [0, \tau].$$

B. Frequency domain

Using frequency measurements as the input data, the QVAR is given by

$$\sigma_Q^2(\tau) = \left\langle [y(t) * h_{Qy}(t)]^2 \right\rangle \quad (10)$$

with (Fig. 3-B)

$$h_{Qy}(t) = \frac{3\sqrt{2}t}{\tau^3} (-t - \tau) \quad t \in [-\tau, 0[$$

$$= \frac{3\sqrt{2}t}{\tau^3} (t - \tau) \quad t \in [0, \tau].$$

In the frequency domain, the QVAR is given by

$$\sigma_Q^2(\tau) = \int_0^\infty S_y(f) |H_{Qy}(f)|^2 df \quad (11)$$

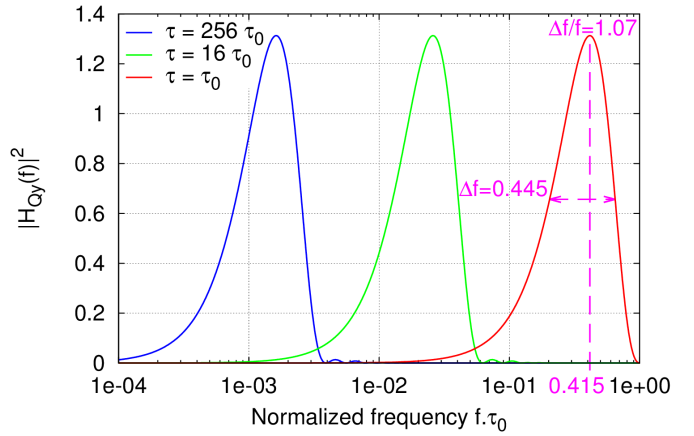


Figure 4. Transfer function of QVAR for 3 values of τ .

Table II
RESPONSES OF QVAR FOR THE DIFFERENT TYPES OF NOISE

| $S_y(f)$ | MVAR(τ) | QVAR(τ) |
|----------------|---|---|
| $h_{-2}f^{-2}$ | $\frac{11\pi^2 h_{-2}\tau}{20}$ | $\frac{26\pi^2 h_{-2}\tau}{35}$ |
| $h_{-1}f^{-1}$ | $\frac{[27 \ln(3) - 32 \ln(2)] h_{-1}}{8}$ | $\frac{2[7 - \ln(16)] h_{-1}}{5}$ |
| $h_0 f^0$ | $\frac{h_0}{4\tau}$ | $\frac{3h_0}{5\tau}$ |
| $h_{+1}f^{+1}$ | $\frac{[24 \ln(2) - 9 \ln(3)] h_{+1}}{8\pi^2 \tau^2}$ | $\frac{3[\ln(16) - 1] h_{+1}}{2\pi^2 \tau^2}$ |
| $h_{+2}f^{+2}$ | $\frac{3h_{+2}}{8\pi^2 \tau^3}$ | $\frac{3h_{+2}}{2\pi^2 \tau^3}$ |

For a linear frequency drift:

$$y(t) = D_1 \cdot t \quad \left\| \quad \frac{1}{2} D_1^2 \tau^2 \quad \left| \quad \frac{1}{2} D_1^2 \tau^2 \right. \right.$$

$H_{Qy}(f)$ being the QVAR transfer function, i.e., the Fourier transform of $h_{Qy}(t)$

$$|H_{Qy}(f)|^2 = \frac{9 [2 \sin^2(\pi\tau f) - \pi\tau f \sin(2\pi\tau f)]^2}{2(\pi\tau f)^6}. \quad (12)$$

The transfer function $|H_{Qy}(f)|^2$, shown in Figure 4, is an octave band pass filter similar to that of the AVAR, but with significantly smaller side lobes. Table II shows the responses to the different types of noise. The same information is shown in Fig. 5.

C. Convergence

For small f , it holds that

$$|H_{Qy}(f)|^2 \approx \frac{3}{(\pi\tau f)^2}. \quad (13)$$

Thus, $\sigma_Q^2(\tau)$ defined in Eq. (11) converges for f^{-2} FM.

At large f , $|H_{Qy}(f)|^2$ decreases as f^{-4} , and $\sigma_Q^2(\tau)$ converges for f^{+2} FM.

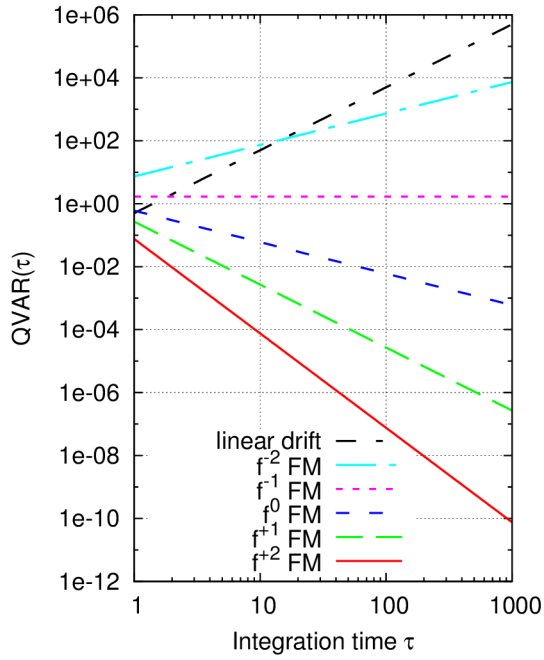


Figure 5. Responses of QVAR for the different types of noise

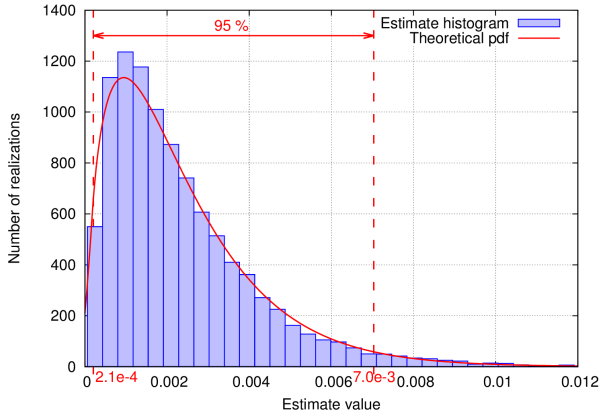


Figure 6. Histogram of 10^4 estimates of the variance

V. EQUIVALENT DEGREES OF FREEDOM

For a general introduction to the problem of the degrees of freedom in the two-sample variance, the reader can refer to [4].

As done with the other variances, we assume that the QVAR estimates are approximately χ^2 distributed

$$\tilde{\sigma}_Q^2(\tau) = \alpha \chi_n^2 \quad (14)$$

where α is a scale coefficient, and n is the Equivalent Degrees of Freedom (EDF). The mathematical expectation and the variance of a χ^2 distribution are proportional,

$$\mathbb{E}\{\chi_n^2\} = n \quad (15)$$

$$\mathbb{V}\{\chi_n^2\} = 2n. \quad (16)$$

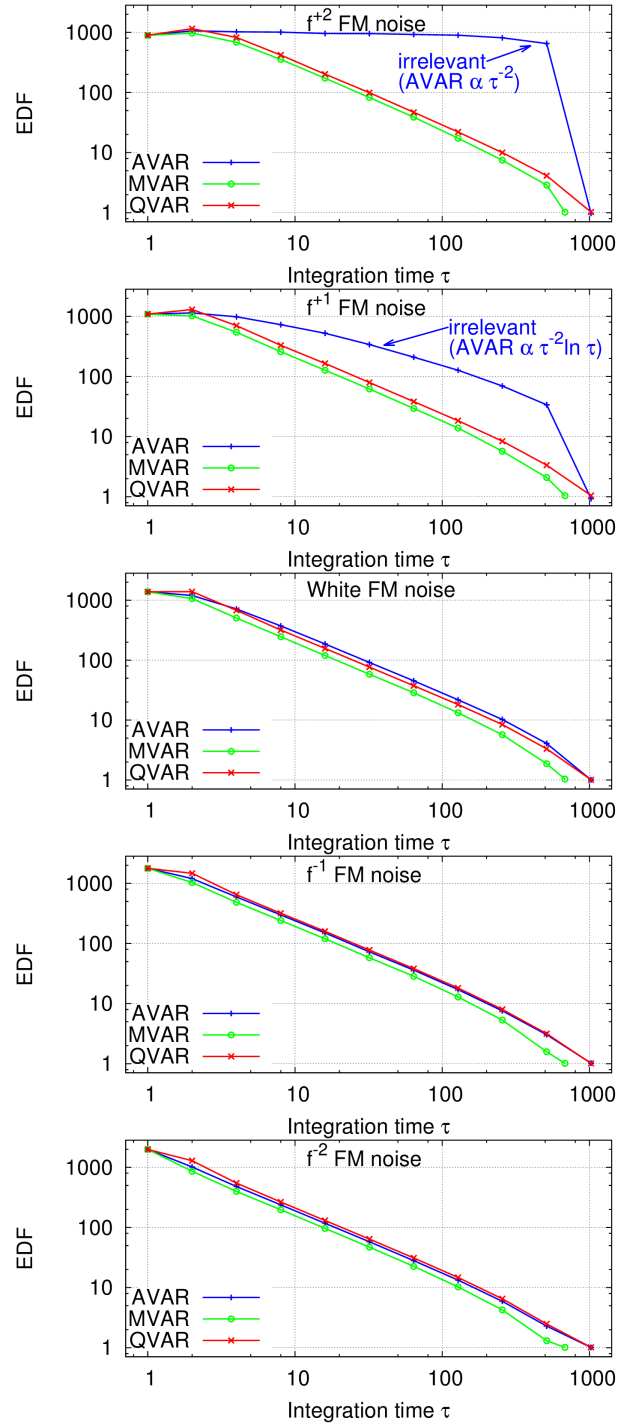


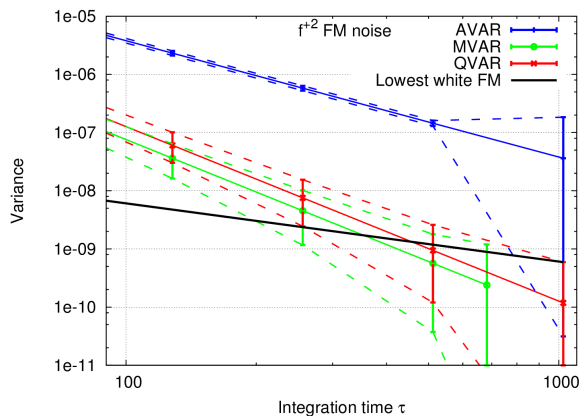
Figure 7. EDF of AVAR, MVAR and QVAR for different types of noise and $N = 2048$, $\tau_0 = 1$ s

The fractional dispersion of the QVAR estimates is given by

$$\frac{\Delta \tilde{\sigma}_Q^2(\tau)}{\tilde{\sigma}_Q^2(\tau)} = \frac{\sqrt{\mathbb{V}\{\tilde{\sigma}_Q^2(\tau)\}}}{\mathbb{E}\{\tilde{\sigma}_Q^2(\tau)\}} = \frac{\sqrt{2\alpha^2\nu}}{\alpha\nu} = \sqrt{\frac{2}{n}}. \quad (17)$$

Figure 6 shows the histogram distribution in the case of 10^4 realizations.

A: White FM noise



B: Frequency drift

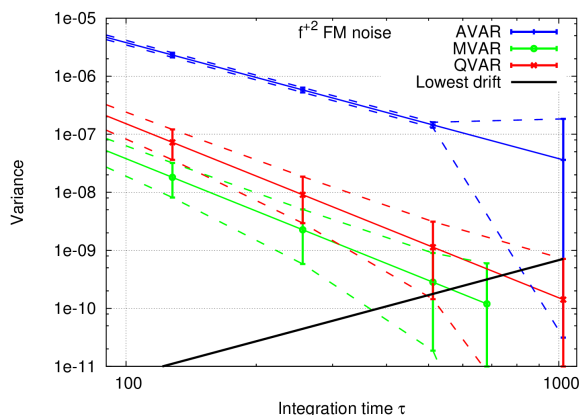


Figure 8. Detection of white FM noise and drift in presence of white PM noise

Figure 7 shows the EDF in a typical representative case, where $N = 2048$. For f^2 and f FM noise (white and flicker PM noise), the AVAR is of little interest because it rejects the background proportionally to $1/\tau^2$ and $1/\tau^2 \ln \tau$, instead of $1/\tau^3$. For all the noise types shown, the QVAR has higher EDF than the MVAR, which is desirable. For the f and f^2 noise types, the QVAR is substantially equivalent to the AVAR.

VI. DETECTION OF WHITE FM NOISE AND DRIFT

Comparing the variances, the capability to detect white FM noise and drift in the shortest time τ , for a given white PM noise (instrument background) is a relevant criterion. The latter can also be expressed as the lowest white FM noise and drift that can be detected in a given τ .

The white FM noise is present in all atomic standards, and the drift is ubiquitous.

Figure 8 A shows a variance plot with PM noise (instrument background), the error bars at 95% confidence level, and a white FM noise (black line). Figure 8 B shows the same variance plot, with a drift (black line). The FM noise (or the drift) is detected with a probability of 95% when the upper point of the error bar hits the FM noise (drift) line. In both cases the MVAR wins.

VII. EXAMPLE OF APPLICATION

Let us consider a time interval analyzer that receives a perfect reference at 1 MHz at the ‘stop’ (time stamp) input, and the 10 MHz output from a H maser at the ‘start’ input. In this condition, the maser phase time is sampled at a rate equal to $1/\tau_0 = 1$ MHz. We assume that each time-interval measurement is affected by white noise (instrument background) with $\sigma_x = 10$ ps. From Table I, the background translates into $\sigma_y = 3.5 \times 10^{-14}$ at $\tau = 1$ s, decreasing as $\tau\sqrt{\tau}$. For comparison, the typical noise of a H maser is $\sigma_y = 10^{-13}$ at $\tau = 1$ s, decreasing as $1/\sqrt{\tau}$. Thus, the Ω counter implemented with such time interval analyzer is in principle sufficient to monitor the maser, out of the box, with no dedicated down-conversion hardware.

ACKNOWLEDGEMENTS

This work is supported by the ANR Programme d’Investissement d’Avenir in progress at the TF Departments of Femto-ST Institute and UTINAM (Oscillator IMP, First-TF and Refimeve+), and by the Région de Franche Comté.

REFERENCES

- [1] C. A. Greenhall, “A method for using time interval counters to measure frequency stability,” *IEEE Trans. Ultras. Ferroelec. Freq. Contr.*, vol. 36, pp. 478–480, Sept. 1989.
- [2] C. A. Greenhall, “The third-difference approach to modified Allan variance,” *IEEE Trans. Instrum. Meas.*, vol. 46, pp. 696–703, June 1997.
- [3] E. Rubiola, “On the measurement of frequency and of its sample variance with high-resolution counters,” *Rev. Sci. Instrum.*, vol. 76, May 2005. Also arXiv:physics/0411227, Dec. 2004.
- [4] P. Lesage and C. Audoin, “Characterization of frequency stability: uncertainty due to the finite number of measurements,” *IEEE Trans. Instrum. Meas.*, vol. 22, pp. 157–161, June 1973.